First-principles LDA+U calculations of the Co-doped ZnO magnetic semiconductor

Shu-jun Hu,* Shi-shen Yan, Ming-wen Zhao, and Liang-mo Mei
School of Physics and Microelectronics, Shandong University, Jinan, Shandong, 250100, People's Republic of China
and State Key Laboratory of Crystal Materials, Shandong University, Jinan, Shandong, 250100, People's Republic of China
(Received 30 November 2005; revised manuscript received 20 April 2006; published 13 June 2006)

Electronic structure of $Co_xZn_{1-x}O$ magnetic semiconductor was investigated by means of density functional calculations using local density approximation (LDA) and LDA+U schemes. The Hubbard U_{Co} implemented in the calculation was determined by means of constrained-density-functional calculations in contrast with the early investigating methods which treated the U as an adjustive parameter. The antiferromagnetic order between nearest-neighbor magnetic ions via the middle O ion was predicted when the intrinsic defects such as O vacancies and Zn interstitials were not taken into account. In sharp contrast with the half-metallic characteristic predicted by most previous theoretical calculations, the $Co_xZn_{1-x}O$ system has semiconductor band structures, which is in good agreement with the results of photoemission spectroscopy. The absence of state near the Fermi level revealed in this paper also accords with the poor conductivity of the on-site samples observed experimentally.

DOI: 10.1103/PhysRevB.73.245205 PACS number(s): 71.27.+a, 75.50.Pp, 71.55.Gs, 75.30.Hx

I. INTRODUCTION

Magnetic semiconductor, which employs the additional spin freedom of electron besides the charge, is one kind of the most promising materials for spintronics. Transition-metal doped wide band gap semiconductors, such as ZnO and GaN in which transition-metal ions are incorporated substitutionally at the Zn or Ga sites, attract much attention due to the theoretical prediction[1] that ZnO and GaN are room temperature ferromagnetic magnetic semiconductor when doped with sufficient quantities of carriers and magnetic atoms. During the past years, a large number of papers have been published to discuss the crystal structure, the origin of ferromagnetism and the Curie temperature (T_c) of Co-ZnO. Much effort has been made to engineer the magnetic semiconductors and especially to realize the half-metallic characteristic in which the conduction electrons at the Fermi energy E_F are 100% spin polarized. The half-metallic density of state (HMDOS) at E_F of $Co_xZn_{1-x}O$ was predicted for different doping concentration by using different theoretical approaches within density functional theory (DFT).[2–5] Though a lot of theoretical data have already been reported, the band structure of Co-doped ZnO is still at a preliminary stage. Until now, little progress has been made in preparing such predicted "half-metallic" materials, although the room temperature ferromagnetism in $Co_xZn_{1-x}O$ has been reported by several groups. Even the ferromagnetic characteristic itself is not robust since the controversial results between different groups show that it strongly depends on the preparation method and the shape of the samples. In fact, the predicted HMDOS at E_F contradicts the poor conductivity of the as-prepared $Zn_{1-x}Co_xO$ films.[6,7] Moreover, the high DOS at E_F in half-metallic materials would produce the instability of the band structure due to the Coulomb correlation interaction between transition metal (TM) 3*d* electrons.[8] Additionally, early studies of homogeneous bulk $Zn_{0.9}Co_{0.1}O$ by using photoemission spectroscopy[9,10] showed that, in contrast with the results of previous local density approximation (LDA) band structure calculations, no emission at E_F was found which clearly suggested the semiconductor band structure and the absence of HMDOS at the Fermi level. Previous theoretical predictions based on the traditional investigating scheme deviate from the experimental results and thus a new scheme is needed to fill the gap.

It is well known that LDA calculations fail in predicting the insulating behavior of many transition metal oxides, but producing the metallic ground state. The incorporating of the effective on-site Coulomb interaction, characterized by Hubbard U, between Co 3*d* electrons into LDA calculations[11] brings about considerable improvement in investigating the transition metal oxides. In the case of large doping concentration of Co, Zn atoms would be entirely substituted by cobalt in a large region, forming a lot of Co-O-like clusters in wurtzite structure. The contradiction between the poor conductivity of the as-prepared $Zn_{1-x}Co_xO$ films and the HMDOS predicted theoretically by using LDA calculations is similar to the above case and may be resolved by incorporating the Hubbard U. Moreover, LDA calculation, either treating the Zn 3*d* electron as valence states or not, always gives rise to a higher energy level of the *d* band of the transition elements,[12] as compared to the experimental results.[13] For the ZnO host material, several approaches employing GW[12] or LDA+U[14] methods are available to correct the Zn 3*d* location. However, in previous theoretical researches Hubbard U was always treated as an adjustive parameter with equivocal meaning. Considering the above research work background one careful investigation of $Co_xZn_{1-x}O$ in LDA+U scheme is necessary.

In this paper we have implemented the v-ESPRESSO software package,[15] with the capability of *calculating* and *implementing* Hubbard U, to investigate the electronic structure of $Co_xZn_{1-x}O$. Calculated results show that: (1) without additional carriers Co atoms favor antiferromagnetic coupling through oxygen in LDA+U scheme; (2) semiconductor band structures were obtained rather than half-metallic characteristic predicted by previous theoretical calculations. Moreover, the absence of state near the Fermi level accords with the poor conductivity of the on-site samples, and the

band structures are consistent with the photoemission spectroscopy.

The paper is organized as follows. In the next section we will discuss the computational details including the method to calculate the Hubbard U_{Co} involved in the LDA+U functional. In Sec. III the calculation results of $Co_xZn_{1-x}O$ system in different configurations will be reported. Finally, some discussion will be given.

II. COMPUTATIONAL DETAILS

The supercell of wurtzite ZnO was firstly optimized to construct the larger doped system. Brillouin Zone integrations were performed by using 4*4*4 Monkhorst and Pack special point grids[16–19] and Methfessel and Paxton smearing technique[20] with a smearing width of 0.005 Ry. The wave functions were expanded in plane waves up to a cutoff energy of 40 Ry and 200 Ry for charge density and potential. Gradient corrected exchange-correlation functional and Hubbard U_{Zn} were used to obtain a fairly good location of Zn 3*d* band. Generalized gradient approximation (GGA) functional in the form of Perdew-Burke-Ernzherof[21] (PBE) was employed here with semicore *d* state and nonlinear core correction for Co atoms.

Using the integer multiples representation of the primitive lattice vectors $\mathbf{a}_1$, $\mathbf{a}_2$, and $\mathbf{a}_3$ of the wurtzite structure, a 2*2*1 supercell containing 16 atoms was used to calculate the parameter U_{Co}. We found that the force and stress of doped systems change little compared to the host material and further coordinate optimization of the doped system was therefore unnecessary. Two Co ions substitute the nearest neighboring cation sites in the 2*2*1 supercell corresponding to the doping concentration of 25 at. %, where Co atoms are either aligned along $\mathbf{a}_1$ direction (represented by C-1 configuration) on the hexagonal plane or along $\mathbf{a}_3$ (**c** axis) direction (represented by C-2 configuration), as shown in Fig. 1 inset. By doubling the 2*2*1 supercell to the $\mathbf{a}_1$ direction, two Co atoms are positioned in the nearest neighboring sites or in the separate Co-O-Zn-O-Co configurations along $\mathbf{a}_1$, named C-3 and C-4 respectively, corresponding to the doping concentration of 12.5 at. %. Another two configurations C-5 and C-6 are defined in the analogous way by doubling the 2*2*1 supercell to the vertical $\mathbf{a}_3$ direction. These six configurations are investigated by calculating the total energy to get the ground magnetic coupling state and detailed band structure of C-1 and C-2 are presented in this paper.

The Hubbard U_{Co} was determined by means of constrained-density-functional calculations.[22] The total energy as a function of the localized-level occupations of the cation sites q_I is shown in Eq. (1)

$$E[\{q_I\}] = \min_{n(r),\alpha_I} \left\{ E[n(r)] + \sum_I \alpha_I (n_I - q_I) \right\}, \tag{1}$$

where the constraints on the site occupations n_I's are applied by using the Lagrange multipliers α_I's. A converged LDA calculation for the unconstrained system was first performed. Starting from its self-consistent potential, small potential shifts were added on each nonequivalent site and then the variation of the occupations n_I's was computed one by one for all sites in the supercell. Finally the influence of the localized orbital rehybridization, as the second term of Eq. (2), was subtracted

$$U = \left(-\frac{\partial \alpha^I}{\partial q_I} \right) - \left(-\frac{\partial \alpha_I^{KS}}{\partial q_I} \right), \tag{2}$$

where the density response functions are introduced here with respect to the localized perturbations. Moreover, the calculation of a larger supercell to extrapolate the results from the smaller one gives no essential correction. So the 2*2*1 supercell is believed to be large enough to compute the U_{Co}.

The location of Zn 3*d* bands in LDA is so high in energy that LDA overestimates the Zn:3d-O:2p hybridization.[12] In order to correctly describe the hybridization, the location of the 3*d* states was adjusted by using LDA+U calculations. The method mentioned above is invalid to gain the Hubbard U_{Zn} since diagonal elements indicating the Zn sites in Eq. (19) of Ref. 22 are close to zero due to fully occupying of Zn 3*d* states. Subtracting the reciprocal of a nearly zero number from that of another one, shown as the two parts of Eq. (2), amplifies the error of the DFT calculations. Therefore, U_{Zn} was considered as a fitting parameter, U_{Zn}=2 eV, in accordance with the GW method which lowers the Zn 3*d* states by about 1 eV compared to the LDA results. Figure 1 shows the density of state (DOS) of ZnO calculated in both

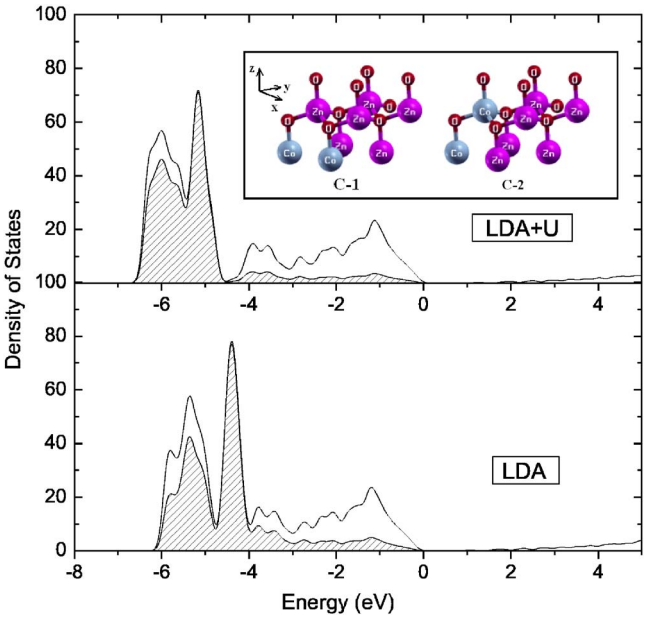

FIG. 1. (Color online) The total density of states (DOS) of the Zn_8O_8 supercell (solid lines, representing the DOS of the pure ZnO), and the partial DOS of the Zn 3*d* states (dashed area). The upper panel shows the DOS image in LDA+U scheme with U_{Zn}=2.0 eV, and the lower panel shows the one in LDA scheme. The energy at the valence-band maximum (VBM) is set to zero. The inset in the upper panel shows two typical configurations of the $Co_2Zn_6O_8$ supercell, where the two Zn ions in Zn_8O_8 supercell of pure ZnO were replaced by two Co ions aligned along $\mathbf{a}_1$ or **c** axis. Blue, pink, and red balls represent Co, Zn, and O atoms, respectively.

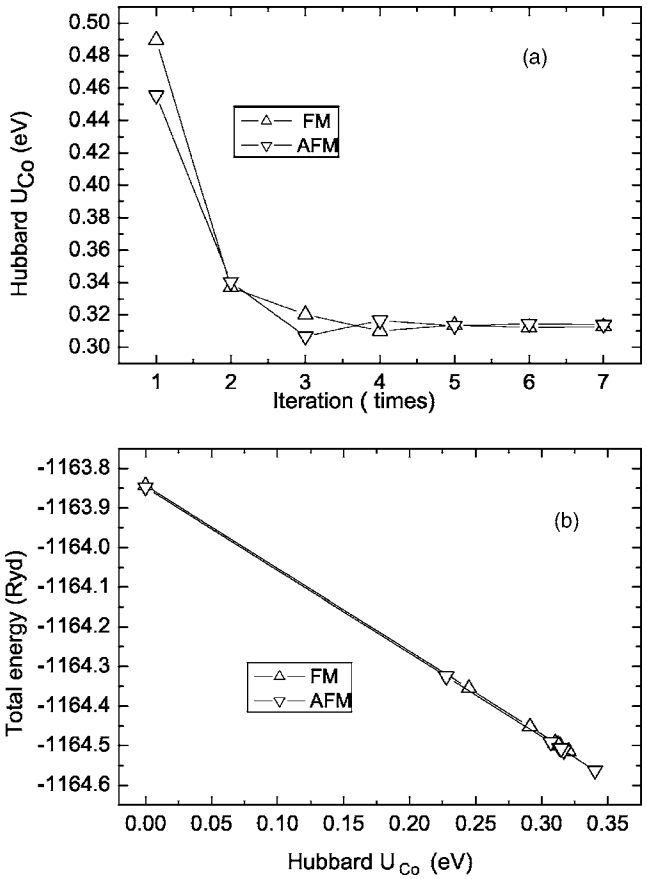

FIG. 2. (a) A diagram showing the process of calculating Hubbard U_{Co}. The proper U_{Co} will be obtained after an internal consistency has been achieved between the previous electronic structures of the supercell configuration employed to calculate the U_{Co} and the following ones calculated by using the obtained U_{Co}, as suggested by Cococcioni and Gironcoli in Ref. 22. (b) The relations between Hubbard U_{Co} and the total energy. In each configuration the total energy is depressed linearly by Hubbard U_{Co} with almost the same slope of the curves.

LDA and LDA+U schemes. Although the energy gap in both schemes is still narrow due to the well-known shortcoming of DFT calculations as compared with the experimental value, the Zn 3*d* states are depressed significantly by the implement of Hubbard U_{Zn}. Therefore, LDA+U scheme is believed to be fairly precise for describing the band hybridization between Zn 3*d* and O 2*p* states.

III. CALCULATED RESULTS AND DISCUSSION

Hubbard U_{Co} was calculated separately in the ferromagnetic (FM) and antiferromagnetic (AFM) electronic spin configurations. The difference in Hubbard U_{Co} is small, ~4 meV, between the two spin configurations after several iteration calculations, as shown in Fig. 2(a). Since Hubbard U represents the Coulomb repulsion between 3*d* electrons at the same site, it slightly depends on the electronic spin configurations. Therefore we employed the average Hubbard U_{Co} of these two spin configurations in our LDA+U calculations. For each configuration total energy is depressed linearly by using Hubbard U_{Co} with almost the *same* slope of the curves [see Fig. 2(b)]. Numerical data including total energy and magnetization are listed in Table I for C-1 and C-2 configurations in FM and AFM coupling states.

The LDA calculations (Table I) show that the AFM state of C-1 configuration is energetically more favorable than its FM state by about 56 meV, whereas, in C-2 configuration, the FM state is energetically more stable than AFM by about 7 meV. However, the calculations by using LDA+U scheme indicate that the AFM states are energetically more stable than FM states in both configurations at about 81 meV and 27 meV, respectively. In the larger supercells containing 32 atoms the nearest neighboring configurations C-3 and C-5 still favor the AFM state by about 40 and 14 meV, respectively. However, the energy differences between FM and AFM states almost vanish for the separate configurations C-4 and C-6. Moreover, the separate configurations are much higher in energy than the nearest neighboring ones C-3 and C-5, about 39 and 24 meV respectively, suggesting the tendency for Co clustering in ZnO and the short range magnetic interactions. The energetic order revealed in LDA+U calculations coincides with the results of previous DFT calculations.[3,4] This is related to the antiferromagnetic coupling between nearest-neighbor Co atoms via oxygen atoms as revealed in $Zn_{1-x}Co_xO$ magnetic semiconductors by different groups.[3,23,24] Although the ferromagnetic semiconductors have been synthesized, the ferromagnetic characteristic itself is not robust.[25] The controversial results reported by different groups show that magnetism strongly depends on the preparation conditions. Experimentalists and theoreticians suggested that the ferromagnetism only occurs in the presence of additional carriers.[3,4,25] In our calculations, the doped systems under study are free from vacancies and interstitial ions, and the E_F locates in the band gap as shown in the following. Such results correspond to a low carrier concentration, which is not high enough to establish the ferromagnetic coupling between the nearest-neighbor Co ions. Therefore we deduce that without any intrinsic defects such as oxygen vacancies and Zn interstitial atoms, Co-doped ZnO semiconductors are characterized by nearest-neighbor antiferromagnetic coupling between magnetic ions via O atoms. However, since the calculated total energy is very close for ferromagnetic and antiferromagnetic orders, the actual $Co_xZn_{1-x}O$ system observed in experiments may stay in different metastable states which show ferromagnetism, antiferromagnetism, or even spin-glass state, depending on the subtle differences in experimental conditions.

Figure 3 shows the spin density of C-1 configuration in a plane containing a Co-O-Co bond. Notable magnetic moment at the oxygen site locating between FM coupled Co atoms is induced by the adjacent Co atoms. This is similar to the theoretical results of the Mn doped ZnSe system.[26] However, the net magnetic moment of the O atom is almost zero in AFM configuration, since the different *p* orbitals of oxygen are polarized distinctly by the nearest Co atoms. In FM configuration absolute magnetic moment of the unit cell is about $6.0\mu_B$ which is slightly larger than $5.7\mu_B$ of AFM configuration and the magnetic contribution from the cation site is about $2.8\mu_B$ in both magnetic states. The smaller magnetic moment of $2.8\mu_B$ distributed by the Co ions, compared

TABLE I. The calculated total energies, total magnetization, absolute magnetization, Hubbard U_{Co} of the $Co_2Zn_6O_8$ supercell, and the total energy differences between FM and AFM states by LDA and LDA+U schemes, respectively.

Configuration	Scheme	Magnetic couple	Total magnetization μ_B/cell	Absolute magnetization μ_B/cell	Total energy Ryd	$\delta E_{FM\text{-}AFM}$ meV
C-1 U=0.3135 eV	LDA	FM	6.02	6.07	−1163.842 521 02	56.12
		AFM	0.00	5.63	−1163.846 647 53	
	LDA+U	FM	6.00	6.04	−1164.500 024 13	80.57
		AFM	0.00	5.61	−1164.505 948 43	
C-2 U=0.3093 eV	LDA	FM	6.03	6.08	−1163.844 894 56	−6.74
		AFM	0.00	5.73	−1163.844 398 66	
	LDA+U	FM	6.00	6.03	−1164.493 200 06	26.76
		AFM	0.00	5.70	−1164.495 167 62	

with the value of $3.0\mu_B$ of isolated Co^{2+} ions, arises from the hybridization between O-2p and Co-3d states. The investigation of different separated configurations in large supercells show the absence of this hybridization in the configurations in which Co ions are not nearest-neighboring aligned. So the noninteger magnetizations of AFM states cannot be interpreted as the schematic diagram of isolated Co^{2+} ions.

The following discussion mainly focuses on the influence of Hubbard U on the band structures of the doping systems. Figures 4(a)–4(d) shows the DOSs of C-1 and C-2 configurations with ferromagnetically coupled Co atoms obtained by using LDA and LDA+U schemes, respectively. The energy of the Fermi level was set to zero. Note that DOSs obtained by using LDA scheme [Figs. 4(b) and 4(d)] are very similar to those reported in previous literatures[3–5] and the difference of DOSs between the C-1 and C-2 is also unnoticeable. In the LDA scheme the exchange and crystal field split the asymmetry of DOSs of spin up and spin down. Co 3d orbitals are split into double e_g states with lower energy and triple t_{2g} states with higher energy by the crystal field in tetrahedral symmetry.[27] Exchange splitting is larger than the crystal field, resulting in the *nearly full-filled* spin-down $e_{g\downarrow}$ states and the empty $t_{2g\downarrow}$ states. The valence-band maximum (VBM) is shifted to the higher energy by 1 eV due to the strong coupling between the majority Co 3d states and the O 2p states. However, the photoemission and transmission spectroscopy show that the band structure of ZnO is not significantly modified by the Co doping,[9,28–30] which is in sharp contrast to the LDA result that no marked band gap exists. Therefore, it is expected that LDA overestimates the $e_{g\downarrow}$ level as well as the coupling between Co 3d and O 2p states, and underestimates the width of the gap.

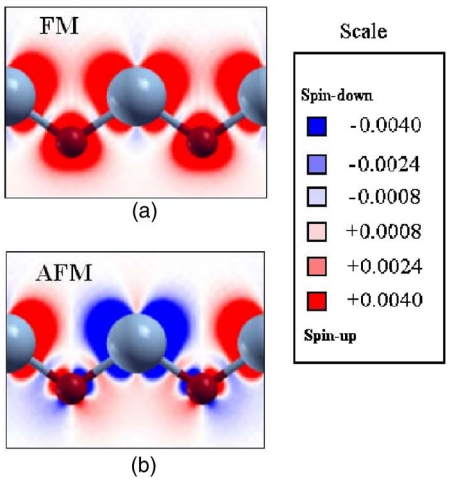

FIG. 3. (Color online) Spin density distribution in real space represented by different color scale for C-1 configuration in LDA+U scheme. In the upper panel (a) two Co atoms are ferromagnetically coupled, inducing the spin polarization of oxygen site significantly. The lower panel (b) shows the AFM configuration without net magnetization. Large balls represent the Co atoms, and the small balls represent the O atoms.

In Figs. 4(a) and 4(c) the band gap is corrected by means of LDA+U. The $e_{g\downarrow}$ states are depressed by 1.5 eV and the E_F locates at the conduction band minimum between $e_{g\downarrow}$ and $t_{2g\downarrow}$ minority states, indicating (i) the n type semiconductors, (ii) non-HMDOS characteristic, and (iii) no emission near the E_F. A higher peak of Co:3d states lies about 1 eV below the E_F in the LDA+U results compared with the photoemission spectroscopy results[9,10] where the peak is around 3 eV. This is due to the well-known shortcoming of LDA approximation which underestimating the band gap of ZnO about ~2 eV. Considering this shortcoming and the position of E_F near the conduction band minimum, the band structure in the LDA+U scheme are in good agreement with the photoemission spectroscopy results.[9,10] Other experimental results that $Co_xZn_{1-x}O$ films are electronic insulators before oxygen vacancies formed by annealing[7] also support the band structures obtained from the present LDA+U calculations.

We also compared the DOSs of the two configurations with Co atoms in the AFM state obtained by using LDA and LDA+U calculations as shown in Figs. 5(a)–5(d). We found that the $t_{2g\uparrow}$ states of these two configurations are merged into the valence band, while the $e_{g\downarrow}$ states are depressed to the top of the valence band. Interestingly if we compare the Co-3d states from the photoemission spectroscopy of FM and AFM samples[9,10] we find that there is no clear difference, which is proved by our calculation results by integrating the spin-up and spin-down states of FM and AFM configurations.

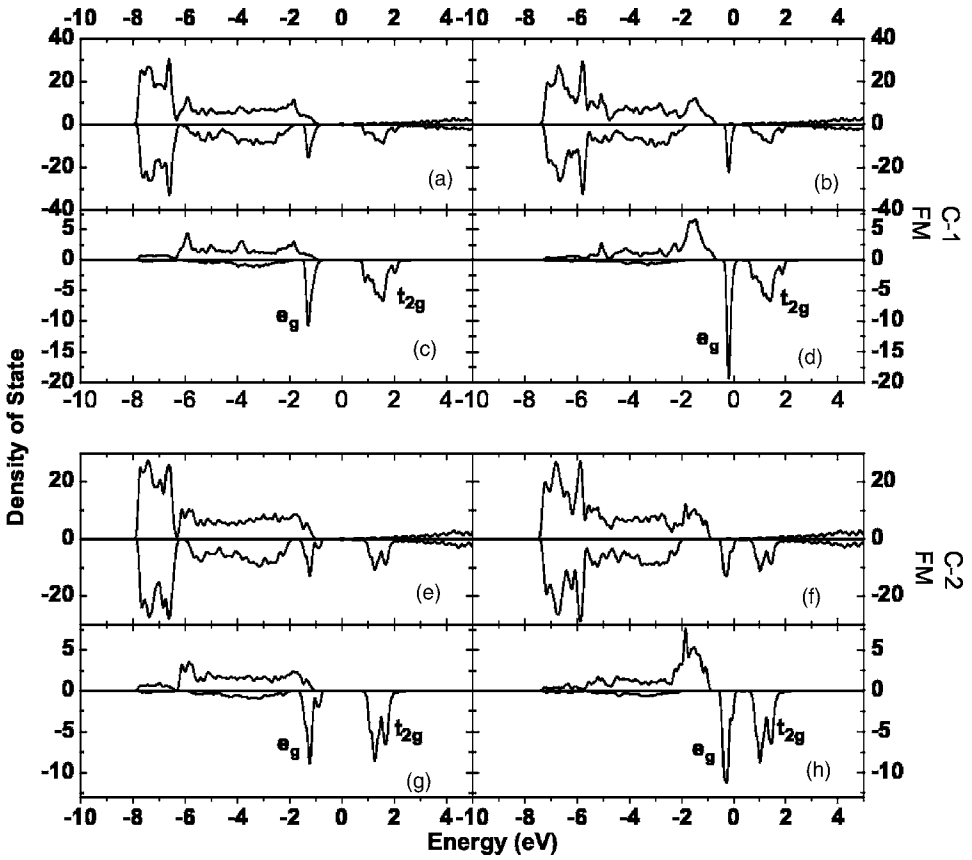

FIG. 4. The total DOS and partial DOS of Co 3*d* states for C-1 and C-2 configuration with two Co atoms ferromagnetically coupled. The energy at the Fermi level is set to zero. The different figures correspond to different configurations and calculation schemes: (a) total DOS of C-1 in LDA+U, (b) total DOS of C-1 in LDA, (c) Co 3*d*-projected DOS of C-1 in LDA+U, (d) Co 3*d*-projected DOS of C-1 in LDA, (e) total DOS of C-2 in LDA+U, (f) total DOS of C-2 in LDA, (g) Co 3*d*-projected DOS of C-2 in LDA+U, (h) Co 3*d*-projected DOS of C-2 in LDA.

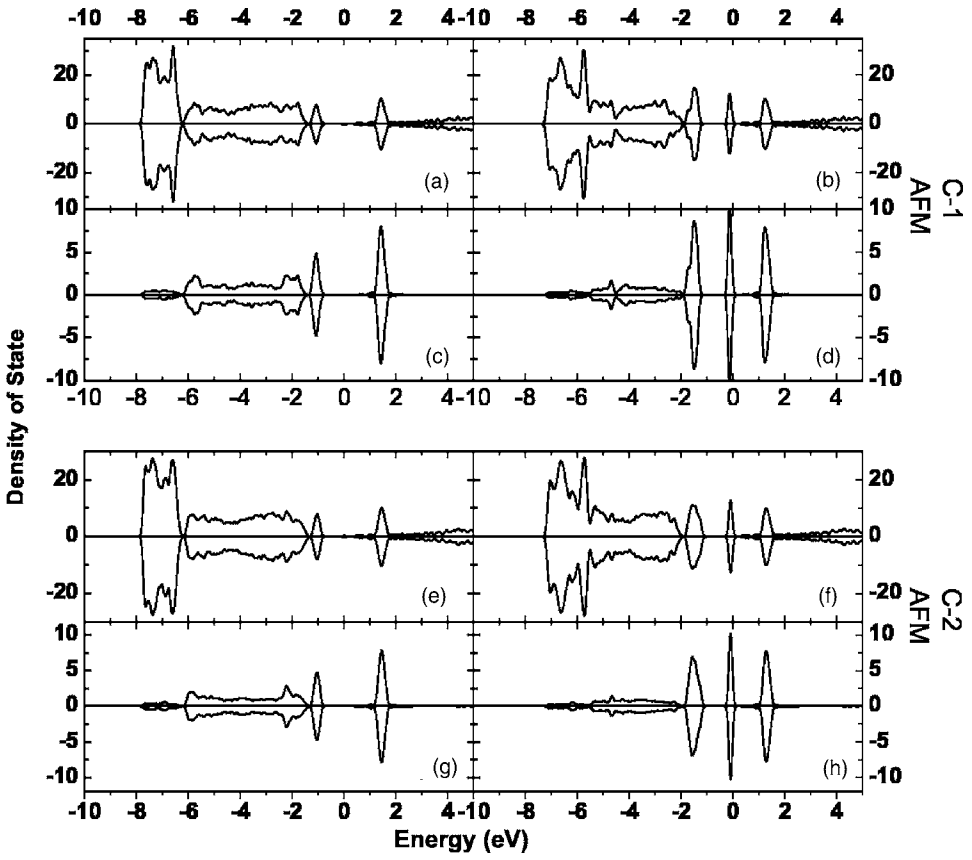

FIG. 5. The total DOS and partial DOS of Co 3*d* states for C-1 and C-2 configuration with two Co atoms in antiferromagnetically coupled state, where the partial DOS of the Co 3*d* states is marked by the dashed area. The energy at the Fermi level is set to zero. The different figures correspond to different configurations and calculation schemes: (a) total DOS of C-1 in LDA+U, (b) total DOS of C-1 in LDA, (c) Co 3*d*-projected DOS of C-1 in LDA+U, (d) Co 3*d*-projected DOS of C-1 in LDA, (e) total DOS of C-2 in LDA+U, (f) total DOS of C-2 in LDA, (g) Co 3*d*-projected DOS of C-2 in LDA+U, (h) Co 3*d*-projected DOS of C-2 in LDA.

It is very interesting to discuss the improvement of our calculations based on the deficiency of LDA functional. Early electron-electron correlation research[31] by using LDA+U formalism indicates that the octahedral CoO_6 cluster, consisting of one Co cation at the center surrounded by six nearest neighbor O anions, can give a good ground state of CoO. In the current calculation the partial DOSs of Co atoms by using both LDA and LDA+U schemes are much similar to the previous theoretical results.[31] There is no obvious difference between the band structures of CoO_6 cluster and Co-O-complex, and therefore the coupling between Co-O-complex and the surrounded atoms is neglected. With the increase of the concentration of Co in ZnO, Co-O-complexes containing one Co atom surrounded by four O atoms will be formed in wider region of the host material. In this case, the LDA calculations cannot give a correct electronic structure of the Co-O-complex system which is supposed to be an analog of correlated system. By analyzing the partial density of state at E_F, we find that DOS at E_F obtained by using LDA functional mainly arises from the O $2p$ and Co $3d$ states. This hybridization gives rise to the *partial occupation* of "$t_{2g\downarrow}$ states" and thus the half-metallic characteristic [as shown in Figs. 4(b) and 4(d)]. So the delocalization of Co $3d$ states originating from the LDA scheme amplifies the hybridization and shrinks the gap incorrectly. It is therefore not surprising that previous LDA calculations were not in agreement with the experimental results that the band structure of ZnO cannot be significantly modified by doping as revealed by the optical transmission spectroscopy.

Band structure improvement induced by the Hubbard U_{Co} is also represented by the change of magnetic moments. In Table I both total and absolute magnetic moments are diminished after introducing the Hubbard U_{Co}. Although the change is small, this result is more reasonable as compared with the experimental magnetic moments of CoO about 2.3–2.8μ_B per Co atom.[32]

IV. CONCLUSIONS

In summary we have investigated the electronic structures and correlation effects of Co-doped ZnO by using the LDA+U scheme. The Hubbard U_{Co} implemented in the calculation was determined by means of constrained-density-functional calculations. The calculations indicate that the $Co_{0.25}Zn_{0.75}O$ system has semiconductor band structures, in sharp contrast with the half-metallic characteristic predicted by the LDA calculations. Moreover, the antiferromagnetic order between nearest-neighbor magnetic ions via the middle O ion (antiferromagnetism) was predicted for the $Co_{0.25}Zn_{0.75}O$ configurations free from intrinsic defects such as O vacancies and Zn interstitials. Band structures obtained by using the LDA+U scheme are in good agreement with many experimental results.

ACKNOWLEDGMENTS

This work was supported by the Project 973 Grant No. 2001CB610603, NSF Grant No. 10234010, 50102019, and 50572053, and New Century Fund for Outstanding Scholars (Grant No. 040634). S. J. Hu would like to thank Q. H. Zhang for the computation support.

*Corresponding author: School of Physics and Microelectronics, Shandong University, Jinan, Shandong, 250100, People's Republic of China. Email: hushujun@mail.sdu.edu.cn; Tel.: +86-531-88375097; Fax: +86-531-88377032.

[1] T. Dietl, H. Ohno, F. Matsukura, J. Cibert, and D. Ferrand, Science **287**, 1019 (2000).
[2] K. Sato and H. Katayama-Yoshida, Sep. Sci. Technol. **17**, 367 (2002).
[3] A. S. Risbud, N. A. Spaldin, Z. Q. Chen, S. Stemmer, and Ram Seshadri, Phys. Rev. B **68**, 205202 (2003).
[4] E.-C. Lee and K. J. Chang, Phys. Rev. B **69**, 085205 (2004).
[5] N. A. Spaldin, Phys. Rev. B **69**, 125201 (2004).
[6] S.-W. Lim, D.-K. Hwang, and J.-M. Myoung, Solid State Commun. **125**, 231 (2003).
[7] A. C. Tuan, J. D. Bryan, A. B. Pakhomov, V. Shutthanandan, S. Thevuthasan, D. E. McCready, D. Gaspar, M. H. Engelhard, J. W. Rogers, Jr., K. Krishnan, D. R. Gamelin, and S. A. Chambers, Phys. Rev. B **70**, 054424 (2004).
[8] M. S. Park and B. I. Min, Phys. Rev. B **68**, 224436 (2003).
[9] S. C. Wi. J.-S. Kang, J. H. Kim, S.-B. Cho, B. J. Kim, S. Yoon, B. J. Suh, S. W. Han, K. H. Kim, K. J. Kim, B. S. Kim, H. J. Song, H. J. Shin, J. H. Shim, and B. I. Min, Appl. Phys. Lett. **84**, 4233 (2004).
[10] M. Kobayashi, Y. Ishida, J. l. Hwang, T. Mizokawa, A. Fujimori, K. Mamiya, J. Okamoto, Y. Takeda, T. Okane, Y. Saitoh, Y. Muramatsu, A. Tanaka, H. Saeki, H. Tabata, and T. Kawai, Phys. Rev. B **72**, 201201(R) (2005).
[11] V. I. Anisimov, J. Zaanen, and O. K. Andersen, Phys. Rev. B **44**, 943 (1991).
[12] S. Massidda, R. Resta, M. Posternak, and A. Baldereschi, Phys. Rev. B **52**, R16977 (1995).
[13] J. E. Jaffe and A. C. Hess, Phys. Rev. B **48**, 7903 (1993).
[14] C. L. Dong, C. Persson, L. Vayssieres, A. Augustsson, T. Schmitt, M. Mattesini, R. Ahuja, C. L. Chang, and J.-H. Guo, Phys. Rev. B **70**, 195325 (2004).
[15] S. Baroni, A. Dal Corso, S. de Gironcoli, P. Giannozzi, C. Cavazzoni, G. Ballabio, S. Scandolo, G. Chiarotti, P. Focher, A. Pasquarello, K. Laasonen, A. Trave, R. Car, N. Marzari, A. Kokalj, http://www.pwscf.org/
[16] A. Baldereschi, Phys. Rev. B **7**, 5212 (1973).
[17] D. J. Chadi and M. L. Cohen, Phys. Rev. B **8**, 5747 (1973).
[18] H. J. Monkhorst and J. D. Pack, Phys. Rev. B **13**, 5188 (1976).
[19] J. D. Pack and H. J. Monkhorst, Phys. Rev. B **16**, 1748 (1977).
[20] M. Methfessel and A. T. Paxton, Phys. Rev. B **40**, 3616 (1989).
[21] J. P. Perdew, K. Burke, and M. Ernzerhof, Phys. Rev. Lett. **77**, 3865 (1996).
[22] M. Cococcioni and S. de Gironcoli, Phys. Rev. B **71**, 035105 (2005).

[23] M. Bouloudenine, N. Viart, S. Colis, J. Kortus, and A. Dinia, Appl. Phys. Lett. **87**, 52501 (2005).
[24] M. Venkatesan, C. B. Fitzgerald, J. G. Lunney, and J. M. D. Coey, Phys. Rev. Lett. **93**, 177206 (2005).
[25] K. Ueda, H. Tabata, and T. Kawai, Appl. Phys. Lett. **79**, 988 (2001).
[26] X. Huang, A. Makmal, J. R. Chelikowsky, and L. Kronik, Phys. Rev. Lett. **94**, 236801 (2005).
[27] For a accurate description of the wurtzite ZnO symmetry, it is inappropriate to use *g* or *u* operation. However, $e_g(e)$ and t_{2g} (t_2) are conventionally used to mark the crystal-field split 3*d* states (see Refs. 4 and 5) since the distortion of the tetrahedron is small. Here the figures accord with the current manner for the purpose of easy understanding.
[28] Z. Jin, T. Fukumura, M. Kawasaki, K. Ando, H. Saito, T. Sekiguchi, Y. Z. Yoo, M. Murakami, Y. Matsumoto, T. Hasegawa, and H. Koinuma, Appl. Phys. Lett. **78**, 3824 (2001).
[29] Z.-W. Jin, T. Fukumura, K. Hasegawa, Y.-Z. Yoo, K. Ando, T. Sekiguchi, P. Ahmet, T. Chikyow, T. Hasegawa, H. Koinuma, and M. Kawasaki, J. Cryst. Growth **237-239**, 548 (2002).
[30] J.-J. Wu, S.-C. Liu, and M.-H. Yang, Appl. Phys. Lett. **85**, 1027 (2004).
[31] P. Wei and Z. Q. Qi, Phys. Rev. B **49**, 10864 (1994).
[32] T. Bredow and A. R. Gerson, Phys. Rev. B **61**, 5194 (2000).